Abdeldjalil ABDELKADER MEKKI[1*], **Abdelkader KANSAB**[1], **Mohamed MATALLAH**[2], **Mouloud FELIACHI**[3]

University of Hassiba Benbouali, Chlef 02000, Algeria, Laboratory L.G.E.E.R (1)
University of Djilali Bounaama, Khemis miliana, Algeria (2)
IREENA-IUT, CRTT, Bd de l'université, BP 406, 44602 Saint-Nazaire cedex, France (3)

doi:10.15199/48.2019.09.16

Fixed-band hysteresis temperature control of induction cooking system

Abstract. *Induction cooking has several advantages: best security, pan heating without thermal inertia, etc.... To further improve the performances of this system, in this paper we present a method that yields a better homogeneity of temperature on the pan's bottom and a good regulation of the temperature. Firstly we propose an inductor structure with four slots containing the coils and we will use the optimization method based on WIPSO technique combined with the 2D FEM method in order to determine the optimal slots distribution and their dimensions .Secondly, a temperature control technique based on the so-called Fixed-band hysteresis (FBHTC) method is used in order to limit the excess temperature on the pan's bottom and to get the desired value suitable for cooking (150-200°C). The optimized structure of the inductor and the regulation of the temperature permit us to achieve our goal.*

Streszczenie. *W artykule zaprezentowano metodę poprawy jednorodności temperatury spodu podgrzewanego indukcyjknie naczynia. Zaproponowano optymalizację konstrukcjio dławika wytwarzająceo pole elektromagnetyczne. Poprawiono też metodę sterowania temperaturą bazując na algorytmie FBHTC - Fixed-band hysteresis.* ***Poprawa właściwości grzejnych i możliwości sterowania temperaturą w kuchniach indukcyjnych***

Keywords: Induction cooking, Finite element method, Fixed-band hysteresis method, Magneto- thermal, Optimization by PSO.
Słowa kluczowe: kuchnie indukcyjne, metoda elementów skończonych, induktor grzejny.

Introduction

Induction cooking provides faster heating, improved thermal efficiency, and low pollution comparable to a gas burner [1].

The principle of induction heating is based on three rules (laws of lentz, lorentz and joule) where the magnetic field created by the inductor induces eddy currents on the pan's bottom and these induced currents cause the heating of the pan by Joule effect [2].

The plan of this work is twofold: Firstly, to obtain an inductor geometry giving a uniform distribution of the temperature on the bottom of the pan. Secondly we propose a technique of control of this temperature. The temperature distribution on the pan's bottom is determined by modelling the magneto thermal phenomena of the system by a 2D finite element method (FEM) and taking into consideration the nonlinearity of the system [3]. In order to have a homogeneous temperature on the pan's bottom, we propose an inductor structure in which the coils are optimally placed in slots (fig. 1).

The optimal inductor geometry giving a uniform distribution of the temperature was obtained in previous researches by using intelligent methods of optimizations (Genetic Algorithms and Neural Networks) [3] [4], but by varying distances di only (Fig.1).The goal of this work is to find an optimal inductor geometry that gives a better uniformity of the temperature distribution than that obtained in [3] [4], by varying both parameters (***di*** and **zi**) simultaneously (Fig.1).

However to achieve such a goal, we model the magneto thermal phenomena of the system by a finite element method (FEM), combined with the improved weight particle swarm optimization method (WIPSO). After obtaining the best distribution of temperature (Fig.8). The latter figure shows that the temperature increases up to 760°C (curie point of pan's material) which exceeds the value of cooking (150°C - 200°C). To have the desired temperature of cooking, we used a regulation's technique of temperature based on of Fixed-band hysteresis (FBH) method [11].

This paper is organised as follows: in section 2, the mathematical modeling and finite element analysisare presented. The temperature distribution from the use of the uniform dimension of slots is determined in section 3. In order to have a uniform temperature distribution, in section 4 the optimal dimensions of slots are calculated from the use of WIPSO technique. The utilisation of the Fixed-Band hysteresis to control the temperature evolution is given in section 5. Finally the conclusion is presented in Section 6

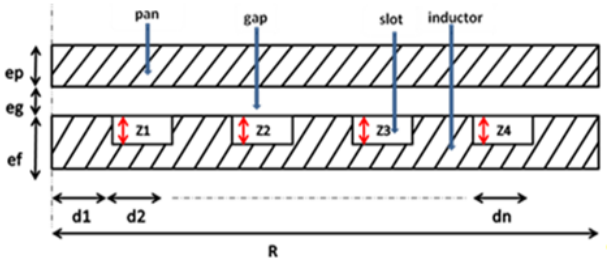

Fig.1. Inductor with four slots

Mathematical Modeling and Finite Elemente Analysis

The aim is to search for a uniform distribution of the temperature on the pan's bottom of the cooking device.

To achieve this aim, it is important to establish the mathematical model of the system. The mathematical modeling of induction cooking devises uses both the magneto-dynamic and the thermal equations. The magneto-dynamic formulation is useful for the determination of the distribution of induced currents generated by the inductor which represent the image of the temperature distribution on the pan's bottom. The eddy current density and the heat source density can be calculated by solving the coupled magneto-dynamic and heat equations. Since the system possesses an axial symmetry, a 2D solution is possible.

Using the magnetic vector potential A, the electromagnetic phenomena are modeled by the well-known magneto-thermal equations ,which are giving by equations (1) to (3) [5-6].

(1) $$j\omega\frac{\sigma\overline{A}}{r}-\frac{\partial}{\partial r}\left(\frac{\nu}{r}\frac{\partial\overline{A}}{\partial r}\right)-\frac{\partial}{\partial z}\left(\frac{\nu}{r}\frac{\partial\overline{A}}{\partial z}\right)=\overline{J}$$

(2) $$\lambda\nabla^2 T+q=\rho_m C_p\frac{\partial T}{\partial t}$$

(3) $$q = \frac{1}{r^2}\sigma\omega^2\overline{A}\overline{A^*}$$

where: $\overline{A}$ - is the magnetic vector potential; r, t - are the radial distance from the axis and the time respectively; ν, σ, ω - are the magnetic reluctivity, the electric conductivity, and the angular frequency, respectively; J ,T - is the current density and the temperature respectively; λ, ρ_m, C_p - are the thermal conductivity, the mass density, and the specific heat, respectively .

It remains to achieve the magneto-thermal model to give boundary conditions. The finite element method 2D-FEM was used for the numerical modeling of both the governing equation (1) and (2) using the following boundary conditions Eq. (4) and (5):

- The boundary conditions in the borders of the pan are of Neumann type conditions equation (4).

(4) $$-\lambda\frac{\partial T}{\partial n} = h(T - T_n)$$

- The boundary conditions for the electromagnetic problem are of :Dirichlet type according to equation (5).

(5) (A = 0)

where : h - is the heat transfer coefficient; Tn - is the ambient temperature.

In this work, we propose that h has a constant value along the radius of the pan[7].
The pan is made of a material of stainless-steel the properties of which are given in [3].

Calculation and Determination of the Temperature Distribution before Optimization

The numerical model is an induction heating pan. The inductor has four slots containing the exciting coils. For the first step we consider that the dimensions (distances di and thicknesses Zi) of the slots and distances between the slots have a uniform distribution as shown in (Fig.2), where di=15.55mm and zi=2mm.The other parameters are shown in table.1, except the value of the current density which is equal to (2.5 *10^6 A/m^2) in this work.

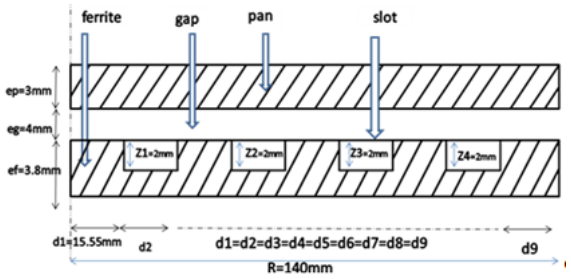

Fig.2. Dimensions of system used

Table 1. Parameters of system

Symbole	Magnitude	Quantity
R	Radius of pan	140mm
e_i	Inductor thickness	3.8mm
e_g	Gap thickness	4mm
e_c	Container thickness	3mm
$d_1, d_2, .d_i$	Distances	15.55mm
e_g	Throat thickness	2mm
μ_f	Ferrite relative permeability	2500
f	Frequency	20*10^3Hz
J	Current density	2.5*10^6 A/m^2
λ	Thermal conductivity	26 W/m*°K
h	Convection coefficient	20 W/m^2°C
ρ_m	Masse density	7700Kg/m^3
C_p	Specific heat	460 J/Kg.°C

The magneto-thermal calculation of our system are given by following steps :

- Step 1: initialization of the electric conductivity, the magnetic permeability, and the temperature σ_0, μ_0, T_0
- Step 2: calculation of the magnetic vector potential (A) by use of equation (1).
- Step 3: calculation of the heat source density is given by equations (2) and (3).
- Step 4: calculation of the temperature T where we use a time step of 10(sec). If $\left(T \le 650\ ^{\circ}C\right)$ go back to step 2 or else go to step 5
- Step 5 : display of the results

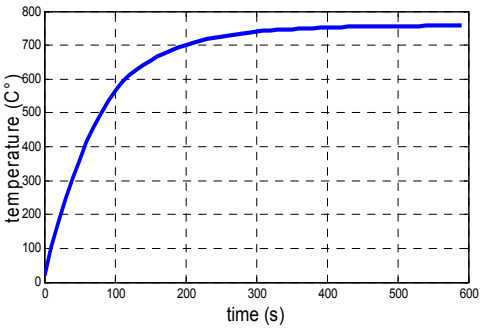

Fig.3. Temperature evolution versus time

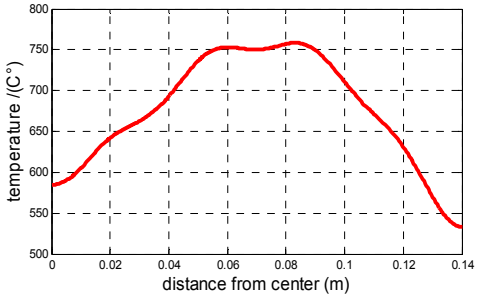

Fig.4.Temperature distribution on pan's bottom

The simulation results obtained are shown in Fig. 3 and Fig. 4. It is clear from Fig. 4 that the temperature distribution on the pan's bottom is not uniform.
Fig. 3 shows that the temperature evolution in the center of the pan's bottom is stopped at the value of 760 C°(curie point of pan's material) [4-6].

Temperature Distribution with Optimization

The objective is to have a homogeneous temperature distribution on the pan's bottom. In this work we suggest the use of The PSO Algorithm to determine the best dimensions of slots (coils) in the inductor by modifying simultaneously the slots' distances (*di*) and their thickness (*zi*). This type of optimization is widely used in nonlinear and complex systems [8].

Problem Presentation

The problem is to find an objective function equation (7) which gives better results. For that, several iterations k of calculation tests must be done in order to determine the optimal geometry of the inductor. The diagram is

summarized in Fig 5. The optimization problem can be formulated as the following equations (6) and (7).

(6) $$MIN\ f_{obj}(d_i, z_i) = f_{obj}(d_1, d_2, \cdots d_9, z_1, z_2, \cdots z_4)$$

(7) $$f_{obj}(d_i, z_i) = \sum_{i=1}^{NT}\left(\frac{T_i - T_f}{T_f}\right) \le \varepsilon$$

where: d_i - is the distances of the slots and the space between the slots; z_i - Is the thiknesses of slots; T_f - is the calculated temperature at each point in the bottom of the pan; T_i - is the desired temperature; NT - Is the number of points in along the bottom of the pan in which the temperature is calculated.

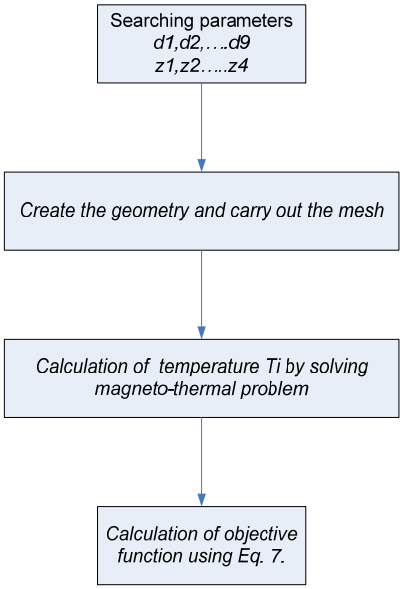

Fig.5. Diagram steps of evaluation objective function

Particle Swarm Optimization

PSO Algorithm has been developed by Kenedy and Eberharet in 1995, and it is based on the movement of a group of animals like a school of fish or a swarm of bees [8-9].

In this technique a swarm (population) comprises a number of particles (individuals) and each particle is represented by a number of parameters to be optimized. Each particle position represents a candidate solution of the optimization problem.

In PSO, each particle in the swarm moves in a D-dimensional space searching for the best position which is defined by an objective function.

In this work, there are thirteen parameters, d_1, d_2, d_3, d_4, d_5, d_6, d_7, d_8, d_9, and z_1, z_2, z_3, z_4, to be estimated, which is equal to the dimension of each each particle.

WIPSO Technique

The PSO Algorithm begins with a randomly generated position of the swarm and each particle moves in the search space with a randomly generated velocity [9].

In this work, the i particle is defined as:

$$\{d_1, d_2, \cdots d_9, z_1, z_2, \cdots z_4\}$$

The position and the velocity vector of each particle at iteration k in the thirteen dimensional spaces are given by the equations (8) and (9) respectively.

(8) $$[d_{1i}, d_{2i}, \cdots d_{9i}, z_{1i}, z_{2i}, \cdots z_{4i}] = \begin{bmatrix} d_{11}^k & d_{21}^k & \cdots & d_{91}^k & z_{11}^k & z_{21}^k & \cdots & z_{41}^k \\ d_{12}^k & d_{22}^k & \cdots & d_{92}^k & z_{12}^k & z_{22}^k & \cdots & z_{42}^k \\ \vdots & \vdots & \vdots & \vdots & \vdots & \vdots & \vdots & \vdots \\ d_{1m}^k & d_{2m}^k & \cdots & d_{9m}^k & z_{1m}^k & z_{2m}^k & \cdots & z_{4m}^k \end{bmatrix}$$

(9) $$[V_{d1i}, V_{d2i}, \cdots V_{d9i}, V_{z1i}, V_{z2i}, \cdots V_{z4i}] = \begin{bmatrix} V_{d11}^k & V_{d21}^k & \cdots & V_{d91}^k & V_{z11}^k & V_{z21}^k & \cdots & V_{z41}^k \\ V_{d12}^k & V_{d22}^k & \cdots & V_{d92}^k & V_{z12}^k & V_{z22}^k & \cdots & V_{z42}^k \\ \vdots & \vdots & \vdots & \vdots & \vdots & \vdots & \vdots & \vdots \\ V_{d1m}^k & V_{d2m}^k & \cdots & V_{d9m}^k & V_{z1m}^k & V_{z2m}^k & \cdots & V_{z4m}^k \end{bmatrix}$$

The positions of each particle are randomly generated, and we need to control them by the following equations (10) to (12).

(10) $$\begin{cases} d_{1\min} \le d_1 \le d_{1\max} \\ d_{2\min} \le d_2 \le d_{2\max} \\ d_{3\min} \le d_3 \le d_{3\max} \\ d_{4\min} \le d_4 \le d_{4\max} \\ d_{5\min} \le d_5 \le d_{5\max} \\ d_{6\min} \le d_6 \le d_{6\max} \\ d_{7\min} \le d_7 \le d_{7\max} \\ d_{8\min} \le d_8 \le d_{8\max} \\ d_{9mn} \le d_9 \le d_{9\max} \end{cases}$$

(11) $$\begin{cases} z_{1\min} \le z_1 \le z_{1\max} \\ z_{2\min} \le z_2 \le z_{2\max} \\ z_{3\min} \le z_3 \le z_{3\max} \\ z_{4\min} \le z_4 \le z_{4\max} \end{cases}$$

(12) $$R_{\min} \le sum(d_{1\ldots\cdots 9}) \le R_{\max}$$

The position giving the best fitness value at iteration (k) of the each particle is saved and represented as:

$$\{pbestd_{1i}^k, pbestd_{2i}^k, \ldots pbestd_{9i}^k, pbestz_{1i}^k, pbestz_{2i}^k, \ldots pbestz_{4i}^k\}$$

The best position giving the best values among all particles in the swarm at iteration (k) is represented by:

$$\{Gbestd_{1i}^k, Gbestd_{2i}^k, \cdots Gbestd_{9i}^k, Gbestz_{1i}^k, Gbestz_{2i}^k, \cdots Gbestz_{4i}^k\}$$

To improve the quality of the solution and the convergence characteristics, the standard PSO technique is modified by the use of the time varying acceleration coefficient, and the time varying inertia weight factor [10].the updated position and velocity of each particle of WIPSO can be expressed by equations (13) and (14).

(13) $$V_{ij}^{k+1} = w_{new} * V_{ij}^k + C_1 * rand_1 * \left(pbest_{ij}^k - X_{ij}^k\right) + C_2 * rand_2 * \left(Gbest_j^k - X_{ij}^k\right)$$

(14) $$X_{ij}^{k+1} = X_{ij}^k + V_{ij}^{k+1}$$

where: V_{ij}^k - is the velocity of particle i at iteration k; ω - is the inertia weight; C_1 , C_2 - are the acceleration coefficients; $rand_1$, $rand_2$ - are random numbers between 0 and 1; X_{ij}^k - is the position of particle i at iteration k; $pbest_{ij}^k$ - is the Best position of particle i at iteration k; $Gbest_j^k$ - is the Best position of the swarm until iteration k.

At each time step, the position and the velocity of each particle i are updated by evaluating the objective function and comparing between the new solution (best position) with the old $Pbest$ (the best position for the i particle at iteration (k-1)) and $Gbest$ (the best position of the swarm at iteration (k-1))[9-10].

The weighting function is calculated as :

(15) $$\omega = \omega_{\max} - \frac{\omega_{\max} - \omega_{\min}}{iter_{\max}}$$

(16) $$\omega_{new} = \omega_{\min} + \omega * rand_3$$

(17) $$C_1 = C_{1\max} - \frac{C_{1\max} - C_{1\min}}{iter_{\max}} * iter$$

where: $\omega_{\max}$ $\omega_{\min}$ - are the maximal and the minimal weight values respectively; $ietr_{\max}$ $ietr_{\min}$ - are the maximum number of iterations and the current iteration number respectively; $C_{1\max}$ $C_{1\min}$ - are the maximal and minimal cognitive coefficients respectively, $C_{2\max}$ $C_{2\min}$ - are the maximal and minimal social coefficients respectively; $rand_3$ - is a Random number between 0 and 1.

Proposed Work Implementation

To determine the optimal slots distribution and their dimensions, PSO algorithm has been used and the following steps have been followed for implementation.

- step 1: initialize the population size m, set the maximum iteration $iter_{max}$, inertia weight ω, acceleration constants $C1$, $C2$ and the number of parameter n to be optimized set the parameters of the simulated system as shown in table (1).
- Step 2: randomly generate the initial position and velocity of each particle in swarm as shown in equations (8) to (12).
- Step 3: for each particle parameter, solve the magneto-thermal problem and then evaluate the fitness function (the process of calculation of the fitness function for each particle parameter is shown in Fig.5.)
- Step 4: assign '*Pbest*' as the best fitness values of particle position; assign '*Gbest*' as the best fitness values among all particle
- Step 5: the steps 5-1 and 5-2 are repeated until the termination criteria are achieved , or until the number of iteration reaches its maximum limit

- Step 5-1: At each iteration *k,* the updated velocity and position of *i* particle are given by equations (13) and (14).
- Step 5-2: for each particle *i* evaluate a fitness function (similar to step3). Assign the new *'Pbest'* and *'Gbest'* (similar to step4)

- step 6 : produce the *Gbest* of particles $\{Gbestd_{1i}^k, Gbestd_{2i}^k, \cdots Gbestd_{9i}^k, Gbestz_{1i}^k, Gbestz_{2i}^k, \cdots Gbestz_{4i}^k\}$

and then take them as optimal dimensions of the slots in the inductor which give a uniform temperature distribution on the pan's bottom.

Simulation and results

The proposed method is developed in matlab , and the simulations were done on a computer with Intel (R) Pentium (R) CPU @2.16 GHz 2.16 GHz 2 GB RAM .The parameters of the WIPSO algorithms are shown in table 2.

Table 2. Parameters setting of WIPSO technique

Algorithme	Inertia weight w	Acceleration Coefficients C_1, C_2	Population size
Wipso	$\omega_{\max} = 0.4$ $\omega_{\min} = 0.9$	$C_{1\max} = 2$ $C_{1\min} = 0.1$ $C_{2\max} = 0.1$ $C_{2\min} = 2$	24

The numerical results are achieved after 40 iterations corresponding to about 10 h. with an acceptable error of ε =0.025. The temperature distribution is represented in Fig. 7. After convergence, the WIPSO method gives a homogeneous distribution of the temperature along a ray of the pan. The best dimensions of the slots are shown in table .3, whereas the optimal geometry of the inductor is shown in Fig 6. The evolution of the temperature as a function of time in the centre on the pan's bottom is shown in the Fig 8.

Table 3. Optimal dimensions of slots

Parameters di,zi	(mm)
d1	16.7
d2	18.1
d3	15
d4	16.7
d5	15.5
d6	17.8
d7	10.8
d8	23.1
d9	6.3
Z1	3.2
Z2	2.5
Z3	2.1
Z4	2.5

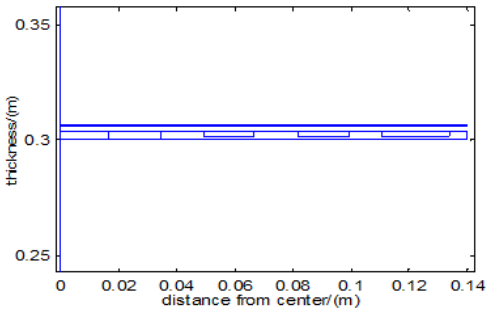

Fig.6. Geometry of the inductor obtained with WIPSO

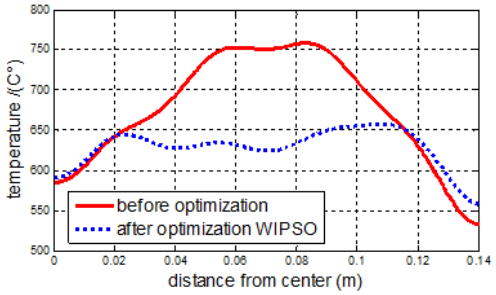

Fig.7.Temperature distribution on pan's bottom

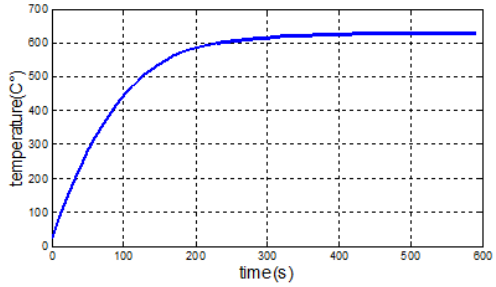

Fig.8. temperature evolution as a function of time in centre of pan

From figure 8, We can see that the temperature obtained exceeds the desired temperature of cooking (150°C-250°C) and increases up to 600°C and more. For this reason, we suggest a control method of temperature based on Fixed-Band hysteresis.

Fixed-Band hysteresis temperature control (FBHTC)

The purpose of using a controller is to control the temperature on the pan's bottom around the value of cooking temperature (150°C -250°C) .In this section we have used the optimal geometry obtained with WIPSO technique to control the temperature evolution versus time.

After regulation

To control linear systems, a mathematical model (transfer function) is used; for example PID controller.

Concerning nonlinear systems, such as a thermal system, it's difficult to model or represent them by a linear model. In this case, the nonlinear systems may not be properly controlled.

In this work, the induction cooking is complex nonlinear system so, it's not easy to obtain an accurate mathematical model that can be used to adjust the temperature of the pan. For this reason, we use a control system based on the fixed-band hysteresis control [11-12] ,which is represented in Fig 9. and Fig 10, to control the temperature evolution in the pan bottom.

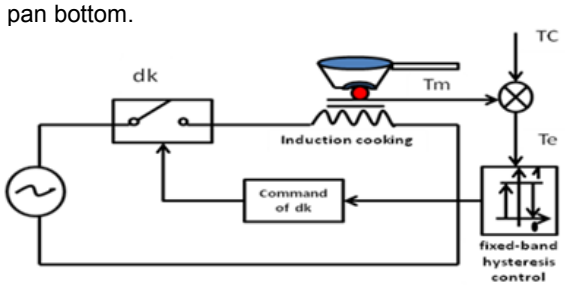

Fig.9. General Scheme of A fixed-band hysteresis temperature control of system

In each time step, the obtained temperature **(Tm)** on the pan's bottom is returned to be compared with the reference desired temperature **(Tc).**

The difference between the temperature obtained and the reference temperature is called the temperature error **(Te).** The latter is compared with the upper band and the lower band of the hysteresis controller to determine the sequence of switching **dk,** as shown in Fig. 11.

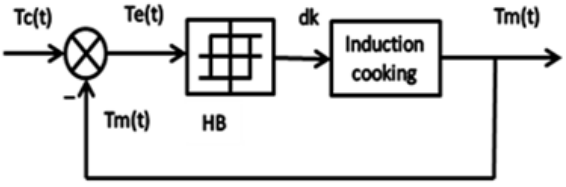

Fig.10. Model used of A fixed-band hysteresis temperature control of system

- in the case where the value of the temperature error reaches the upper value of the band, the switch dk will be activated
- if the value of the temperature error reaches the lower value of the band the switch dk will be deactivated

In this algorithm the band width is kept constant during all the calculation process of the temperature. The algorithm for this technique is given as:

(19) Upper band $T_C(t) = T_M + HB$ if $T_C(t) - T_M(t) \rangle HB$ then dk OFF

(20) Lower band $T_C(t) = T_M - HB$ if $T_C(t) - T_M(t) \langle HB$ then dk ON

Tc - the reference temperature; Tm - temperature obtained; HB - is the band width

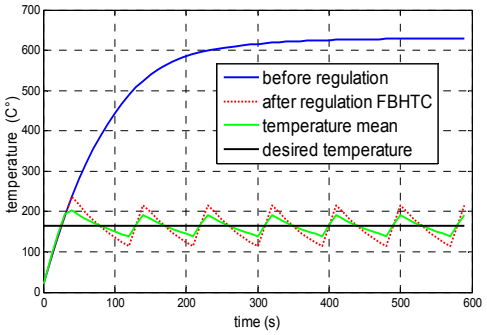

Fig.11.Temperature evolution as a function of time after regulation

The results of the regulation are shown in Fig 11, where we see that the use of Fixed-Band hysteresis control assures a good regulation, and limits the temperature variation within the band used for cooking, which oscillates between 160 C° and 220 C°.

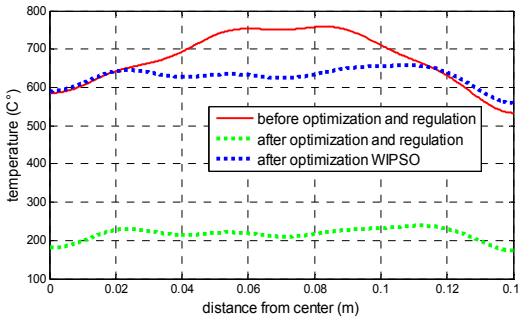

Fig.12.Temperature distribution after optimization and regulation

Figure 12, shows that after optimization and regulation of the temperature, we have the desired homogeneous temperature on the pan's bottom corresponding to the cooking temperature range.

Conclusion

In this paper we presented a way to achieve a uniform distribution of the temperature of an induction heating cooking system. A finite element method is used to analyse the magneto-thermal problem and a PSO technique is employed on the induction-heating cooking device, to optimize the structure of the slots in the inductor.

A technique of regulation has been adopted for the work using the Fixed-Band hysteresis temperature control to find out the adapted temperature for the induction cooking system.

The main feature of this FBHC method is the simplicity of implementation, and its robustness.

This study shows that the proposed technique (**FBHTC**) gives a good regulation of the temperature which is in the cooking range, i.e. between 150-250 C.

Authors

Abdeldjalil abdelkader mekki *was born in khemis miliana, Algeria, in 1986. He received the engineer Degree, in Electrical Engineering from the University of khemis miliana, Algeria, in 2014. He is currently working towards his Ph.D. in the LGEER Laboratory (Laboratoire Génie Electrique et Energies Renouvelables). His research interest includes intelligent control strategies, electrical machine drives, renewable energies, optimization and systems modeling and control* ***Email:*** ***a.abdelkadermekki@univ-chlef.dz***

Abdelkader Kansab *was born in Mazouna, Algeria, in 1964. He received the doctorat degree, in Electrical Engineering from the University of Sciences and technology of Oran, Algeria, in 2008. He is currently working as an Associate Professor at the university of chlef and is a member in the LGEER Laboratory (Laboratoire Génie Electrique et Energies Renouvelables). His research interests include modeling and optimization in Electromagnetic systems and devices. Email: a.kansab@univ-chlef.dz*

Mohamed Matallah *was born in Arib, Algeria, in 1961. He received his PhD in Electrical Engineering in 1991 at the University of Swansea, UK. He is currently working as an Associate Professor at the University of Khemis-Miliana, Algeria, and is a member of The LESI (Energies and Intelligent Systems) Laboratory. His research interests include Electrical Discharges in Gases and Electromagnetic systems and devices. Email : m.matallah@univ-dbkm.dz*

Mouloud Feliachi *is Professeur emérite, IUT de ST-NAZAIRE , University de Nantes . responsable du Réseaux de Recherche en inductique " inductics-Net" . labo recherché : IREENA Equipe : MDE*
http://www.univ-nantes.fr//feliachi-m

REFERENCES

[1] Meng LC, Cheng KWE , Luk PCK. (2012). Field analysis of an induction cooker with square 9-coil system by applying diverse exciting patterns. *Power Electronics, Machines and Drives (PEMD 2012). 6th IET International Conference on*. IET. 2012.

[2] Acero J, Hernandez PJ, Burdío J M , Alonso R, Barragdan L A. (2005). Simple resistance calculation in litz-wire planar windings for induction cooking appliances. *IEEE Transactions on magnetics*. *41*(4): 1280-1288.

[3] Kanssab A, Zaoui A, Feliachi M. (2012). Modeling and optimization of induction cooking by the use of magneto-thermal finite element analysis and genetic algorithms. *Frontiers of Electrical and Electronic Engineering*, *7*(3): 312-317.

[4] Allaoui F, Kanssab A, Matallah M, Zaoui A, Feliachi M. (2014). Modelling and Optimization of Induction Cooking by the use of Magneto-thermal Finite Element Analysis and Neural Network. In *Materials Science Forum*. Trans Tech Publications. 792: 251-259.

[5] Terrail Y Du, Sabonnadiere JC, Masse P, Coulomb J L. .(1984). Nonlinear complex finite elements analysis of electromagnetic field in steady state AC devices. IEEE Transactions on Magnetics. 20(4): 549–552.

[6] Féliachi M, Develey G. (1991). Magneto-thermal behavior finite element analysis for ferromagnetic materials in induction heating devices. IEEE Transactions on Magnetics. 27(6): 5235–5237.

[7] Byun J K, Choi K, Roh H S, Hahn S Y. (2000). Optimal design procedure for a practical induction heating cooker. *IEEE Transactions on Magnetics*, *36*(4), 1390-1393.

[8] Shi Y, Eberhart RC. (1999). Empirical study of particle swarm optimization. In *Proceedings of the 1999 Congress on Evolutionary Computation-CEC99 (Cat. No. 99TH8406),IEEE.* 3: 1945-1950.

[9] Sankardoss V, Geethanjali P. (2017). PMDC Motor Parameter Estimation using Bio-Inspired Optimization Algorithms. *IEEE Access*. 5 : 11244-11254.

[10] Kavitha K, Neela R. (2016). Comparison of BBO, WIPSO & PSO Techniques for the Optimal Placement of FACTS Devices to Enhance System Security. *Procedia Technology*. 25: 824-837.

[11] Belloum K D, Moussi A. (2008). A fixed band hysteresis current controller for voltage source AC chopper. *World Academy of Science Engineering and Technology*. 45 :350-356..

[12] Vahedi H, Pashajavid E, Al-Haddad K. (2012). Fixed-band fixed-frequency hysteresis current control used In APFs. In *IECON 2012-38th Annual Conference on IEEE Industrial Electronics Society*,IEEE. pp. 5944-5948.